Title

Intermittent Hypoxia and Hypercapnia Accelerate Atherosclerosis, Partially via Trimethylamine-Oxide

Journal

American Journal of Respiratory Cell and Molecular Biology, 57(5)

ISSN

1044-1549

Authors

Xue, Jin

Zhou, Dan

Poulsen, Orit

et al.

Publication Date

2017-11-01

DOI

10.1165/rcmb.2017-0086oc

Peer reviewed

ORIGINAL RESEARCH

Intermittent Hypoxia and Hypercapnia Accelerate Atherosclerosis, Partially via Trimethylamine-Oxide

Jin Xue[1], Dan Zhou[1], Orit Poulsen[1], Toshihiro Imamura[1], Yu-Hsin Hsiao[1], Travis H. Smith[1], Atul Malhotra[2], Pieter Dorrestein[1,3,4], Rob Knight[1,4,5], and Gabriel G. Haddad[1,3,5,6]

Departments of [1]Pediatrics, [2]Internal Medicine, and [3]Neurosciences, School of Medicine, [4]School of Pharmacy and Pharmaceutical Sciences, and [5]Department of Computer Sciences and Engineering, School of Engineering, University of California San Diego, La Jolla, California; and [6]The Rady Children's Hospital, San Diego, California

Abstract

Obstructive sleep apnea (OSA) is a common disorder characterized by intermittent hypoxia and hypercapnia (IHC) during sleep. OSA has been shown to be a risk factor for atherosclerosis, but the relation of IHC to the induction or progression of atherosclerosis is not well understood. To dissect the mechanisms involved, we compared atherosclerotic lesion formation in two mouse models, i.e., apolipoprotein E *(ApoE)* and low density lipoprotein receptor *(Ldlr)*–deficient mice, with or without IHC exposure. Ten-week-old $ApoE^{-/-}$ or $Ldlr^{-/-}$ mice were fed a high-fat diet for 4 or 8 weeks while being exposed to IHC for 10 hours/day or room air (RA) for 24 hours/day. *En face* lesions of the aorta, aortic arch, and pulmonary artery (PA) were examined. Moreover, 3,3-dimethyl-1-butanol (DMB), an inhibitor of microbial trimethylamine (TMA) production, was used to determine the contribution of TMA-oxide (TMAO) to IHC-induced atherosclerosis. Eight weeks of IHC exposure expedited the formation of atherosclerosis in both the PA and aortic arch of $ApoE^{-/-}$ mice, but only in the PA of $Ldlr^{-/-}$ mice ($ApoE^{-/-}$ PA 8 wk, IHC 35.4 ± 1.9% versus RA 8.0 ± 2.8%, $P <$ 0.01). The atherosclerotic lesions evolved faster and to a more severe extent in $ApoE^{-/-}$ mice as compared with $Ldlr^{-/-}$ mice (PA IHC 8 wk, $ApoE^{-/-}$ 35.4 ± 1.9% versus $Ldlr^{-/-}$ 8.2 ± 1.5%, $P < 0.01$). DMB significantly attenuated but did not totally eliminate IHC-induced PA atherosclerosis. Our findings suggest that IHC, a hallmark of OSA, accelerates the progression of atherosclerosis in the aorta and especially in the PA. This process is partly inhibited by DMB, demonstrating that microbial metabolites may serve as therapeutic targets for OSA-induced atherosclerosis.

Keywords: atherosclerosis; intermittent hypoxia and hypercapnia; microbes; obstructive sleep apnea

Clinical Relevance

Obstructive sleep apnea is a common sleep disorder that is characterized by intermittent hypoxia and hypercapnia (IHC) during sleep and has been shown to be an independent risk factor for atherosclerosis. However, the experimental time course, the susceptibility of the vascular beds, and the mechanistic links between IHC and the development of atherosclerosis are not well understood. Our current study shows that IHC accelerates the progression of atherosclerosis in both $ApoE^{-/-}$ and $Ldlr^{-/-}$ mice in the aorta and especially in the pulmonary arteries. This process is partly inhibited by a nonlethal microbial trimethylamine (TMA) lyase inhibitor, suggesting the involvement of microbes and their metabolites TMA and TMA-oxide. These metabolites may serve as potential therapeutic targets for the prevention and treatment of obstructive sleep apnea–induced atherosclerosis.

(Received in original form March 3, 2017; accepted in final form June 20, 2017)

This work was supported by National Institutes of Health grants 5P01 32573 (G.G.H.) and K24 HL132105, RO1HL085, and T32 HL134632 (A.M.).

Author Contributions: Conception or design: J.X., D.Z., A.M., P.D., R.K., and G.G.H. Acquisition of data: O.P., T.I., Y.-H.H., and T.H.S. Analysis and interpretation of data: J.X., D.Z., and O.P. Drafting of the manuscript: J.X. and D.Z. Revision and final approval of the manuscript: J.X., D.Z., O.P., T.I., Y.-H.H., T.H.S., A.M., P.D., R.K., and G.G.H.

Correspondence and requests for reprints should be addressed to Gabriel G. Haddad, M.D., Department of Pediatrics, University of California San Diego, 116 Leichtag Building, 9500 Gilman Drive, La Jolla, CA 92093-0735. E-mail: ghaddad@ucsd.edu

This article has a data supplement, which is accessible from this issue's table of contents at www.atsjournals.org

Am J Respir Cell Mol Biol Vol 57, Iss 5, pp 581–588, Nov 2017

Originally Published in Press as DOI: 10.1165/rcmb.2017-0086OC on July 5, 2017
Internet address: www.atsjournals.org

Obstructive sleep apnea (OSA) has been identified as an independent risk factor for various cardiopulmonary diseases (1, 2), which can lead to increased cardiovascular morbidity (3). Clinical studies have shown that the risk of atherosclerosis is associated with OSA severity (4, 5), but the experimental time course, the susceptibility of vascular beds, and mechanistic links between intermittent hypoxia and hypercapnia (IHC, a hallmark of OSA) and the development of atherosclerosis are not well understood.

Atherosclerosis is a complex inflammatory disease and is thought to start with endothelial damage followed by progressive plaque formation inside the arteries. Plaques reduce or completely block blood flow to the tissues and result in various ischemic diseases. Mice deficient in either apolipoprotein E *(ApoE)* (6, 7) or low density lipoprotein receptor *(Ldlr)* (8) are the two most commonly used mouse models for atherosclerosis. Both ApoE and Ldlr play important roles in the clearance of cholesterol and triglyceride-rich lipoprotein particles from the blood. We recently reported that 8 and 16 weeks of IHC exposure remarkably accelerated the formation of atherosclerosis in the pulmonary artery (PA) of $Ldlr^{-/-}$ mice on a high-fat diet (HFD), which was accompanied by hemodynamic changes consistent with early pulmonary hypertension and right-ventricular strain (9). However, IHC did not cause more lesion formation in the aorta after either 8 or 16 weeks of exposure, although the absolute extent of the lesions was increased after 16 weeks. In this work, we further studied the effects of IHC on the formation of atheroma after 4- and 8-week IHC treatments, and compared atherosclerotic lesions in $ApoE^{-/-}$ and $Ldlr^{-/-}$ mice using the same methods.

Emerging research evidence suggests that gut microbes are participants in atherosclerosis development (10–12). Gut microbial trimethylamine (TMA) lyases metabolize dietary choline into TMA, which is oxidized by hepatic flavin monooxygenases and converted into TMA *N*-oxide (TMAO). Blood TMAO levels have been associated with atherosclerotic heart diseases and adverse cardiac events in multiple cohorts (12–17). A structural analog of choline, 3,3-dimethyl-1-butanol (DMB), is a microbial TMA lyase inhibitor. DMB in the drinking water of $ApoE^{-/-}$ mice reduces blood TMAO levels and inhibits the development of atherosclerosis (10). OSA increases the risk for atherosclerotic lesions and is marked by IHC (4, 5). Intermittent hypoxia (IH) was previously reported to alter gut microbiota diversity in a mouse model of sleep apnea (18). Thus, we used DMB to determine whether the same pathophysiology occurs in OSA-induced atherosclerosis.

In this study, we sought to determine whether (*1*) IHC accelerates the progression of atherosclerosis, (*2*) atherosclerotic lesions depend on the vascular system (i.e., the PA or aorta), (*3*) the genetic background of the mice (i.e., $ApoE^{-/-}$ or $Ldlr^{-/-}$) makes a difference in atherogenesis under room air (RA) and IHC conditions on an HFD, and (4) gut microbes contribute to IHC-induced atherosclerosis in a model of OSA. Preliminary results of this study have been previously reported in abstract form (19).

Materials and Methods

Animals

Because mice are resistant to atherosclerosis, we used atherosclerosis-prone, 10-week-old male $Ldlr^{-/-}$ and $ApoE^{-/-}$ mice on a C57BL/6J background (stock numbers 002207 and 002052, respectively; The Jackson Laboratory, Bar Harbor, ME) in this study (8, 20). *Ldlr* and *ApoE* deficiencies were confirmed by PCR according to the vendor's instructions. All animal protocols were approved by the Animal Care Committee of the University of California San Diego and followed the National Institutes of Health *Guide for the Care and Use of Laboratory Animals*.

HFD Treatment

Mice were fed with regular chow consisting of 0.01% cholesterol and 4.4% fat (TD8604; Harlan-Teklad, Madison, WI) until initiation of dietary and IHC treatments. Starting at 10 weeks of age, male mice were provided with an HFD containing 1.25% cholesterol and 21% milk fat (4.5 Kcal/g; TD96121; Harlan-Teklad, Madison, WI) for 4 or 8 weeks while being exposed to either IHC or RA. The body weight of each mouse was measured twice a week. The food intake of the animals in each cage was recorded every week.

IHC Exposure

IHC was maintained in a computer-controlled atmosphere chamber system (OxyCycler; Reming Bioinstruments, Redfield, NY) as previously described (21). Mice were exposed to IHC for short periods (~4 min) of a synchronized reduction of O_2 (from 21 to 8%) and increase of CO_2 (from ~0.5 to 8%) separated by alternating periods (~4 min) of normoxia ($[O_2]$ = 21%) and normocapnia ($[CO_2]$ = ~0.5%), with 1- to 2-min ramp intervals for 10 hours/day during the light cycle, for either 4 or 8 weeks. This treatment protocol mimics the severe clinical condition observed in patients with OSA. Mice that were on the same HFD but in RA were used as controls.

DMB Treatment

DMB nonlethally inhibits TMA production and reduces plasma TMAO levels (10). To evaluate the contribution of microbes and TMAO to IHC-induced atherosclerosis, we added DMB (1%, vol/vol; Sigma-Aldrich, St. Louis, MO) to the drinking water of mice that were fed an HFD and exposed to 8 weeks of IHC.

Quantification of Atherosclerotic Lesions

Atherosclerosis was quantified by computer-assisted image analysis (ImageJ, NIH Image) (22) in Sudan Red-stained en face preparations of the aorta and PAs as previously described (9). Briefly, the heart was perfused with cold PBS plus EDTA, followed by fixation with 4% paraformaldehyde. The entire aorta, pulmonary root, and left and right PAs were dissected out and stained with Sudan Red. The extent of the lesions was quantified by the percentage of lesion area in the total area of the tissue examined using ImageJ. Images of the aortic arch were cropped from the rest of the aorta by measuring the same distance from the bifurcation to the aortic body using photo-editing software (Adobe Photoshop CS6; Adobe Systems Inc., San Jose, CA). All measurements were done by blinded investigators.

Statistical Analysis

Data are presented as means ± SEM. Student's *t* test was employed and $P < 0.05$ was considered statistically significant.

Results

Figure 1 is a schematic illustration of the treatment paradigm (RA, IHC, and DMB).

Impact of IHC on the Formation of Atherosclerosis in *ApoE*$^{-/-}$ and *Ldlr*$^{-/-}$ Mice

After 4 weeks of treatment, atherosclerotic lesions were detected in both the aorta and PA, with the highest level found in the PA of the IHC group of *ApoE*$^{-/-}$ mice. There was no statistically significant difference between IHC-treated *ApoE*$^{-/-}$ mice and RA controls with respect to the aorta, aortic arch, and PA. Similar results were obtained in the *Ldlr*$^{-/-}$ mice (data not shown).

At 8 weeks, IHC treatment resulted in more and larger atherosclerotic lesions as compared with the RA condition, especially in the PA, in both animal models examined. In the *ApoE*$^{-/-}$ mice, significant increases in lesion formation by IHC were observed in the aortic arch (RA 7.0 ± 1.1% versus IHC 16.1 ± 1.9%, $P < 0.01$) and PA (RA 8.0 ± 2.8% versus IHC 35.4 ± 1.9%, $P < 0.01$), but not in the entire aorta (Figures 2A and 2B). Interestingly, this IHC-induced increase in lesion formation was only found to be significant in the PA (RA 2.1 ± 0.2% versus IHC 8.2 ± 1.5%, $P < 0.01$) in the *Ldlr*$^{-/-}$ mice (Figures 3A and 3B). It is not surprising that the lesions in the aorta were mainly located in the aortic arch. The aortic arch is subject to considerable shear force and thus is susceptible to endothelial cell damage, which is the first step in the formation of atherosclerotic lesions.

Along the time course of the treatment (from 4 to 8 wk), we found that the atherosclerotic lesions in the *ApoE*$^{-/-}$ mice evolved with time under both the RA and IHC conditions, but more rapidly in the aortic arch and PA of IHC-exposed mice (Figure 4A). In contrast, in the *Ldlr*$^{-/-}$ mice, we observed an IHC-independent progression of lesions in the aorta and IHC-stimulated lesion formation in the PA (Figure 4B). Intriguingly, the lesions in the PA did not progress, but the lesions in the aorta and aortic arch evolved during the 4- to 8-week period under RA conditions (Figure 4B). These results demonstrated that the aorta, rather than the PA, was affected in *Ldlr*$^{-/-}$ mice on an HFD in RA.

Reduced body weight and high-fat food intake were observed in IHC-treated mice (Figures E1 [*ApoE*$^{-/-}$] and E2 [*Ldlr*$^{-/-}$] in the online supplement).

Comparison of Atherosclerotic Lesion Progression in *ApoE*$^{-/-}$ and *Ldlr*$^{-/-}$ Mice

We further compared the severity of the lesions and the progression rate between *ApoE*$^{-/-}$ and *Ldlr*$^{-/-}$ mice. After 4 weeks of treatment, the PA lesions induced by IHC were significantly larger in *ApoE*$^{-/-}$ mice than in *Ldlr*$^{-/-}$ mice (PA IHC 4 wk, *ApoE*$^{-/-}$ 8.8 ± 1.9% versus *Ldlr*$^{-/-}$ 3.8 ± 0.7%, $P < 0.05$; Figure 4). The extent of IHC-induced PA lesions at 4 weeks in *ApoE*$^{-/-}$ mice was comparable to the level at 8 weeks in *Ldlr*$^{-/-}$ mice (PA IHC, *ApoE*$^{-/-}$ 4 wk 8.8 ± 1.9% versus *Ldlr*$^{-/-}$ 8 wk 8.2 ± 1.5%, $P > 0.05$; Figure 4). After 8 weeks of treatment, the IHC-induced lesions were all significantly larger in the aorta, aortic arch, and PA in *ApoE*$^{-/-}$ mice than in *Ldlr*$^{-/-}$ mice (IHC 8 wk, aorta: *ApoE*$^{-/-}$ 5.6 ± 0.7% versus *Ldlr*$^{-/-}$ 2.8 ± 0.4%, $P < 0.01$; aortic arch: *ApoE*$^{-/-}$ 16.1 ± 1.9% versus *Ldlr*$^{-/-}$ 9.8.±1.2%, $P < 0.05$; PA: *ApoE*$^{-/-}$ 35.4 ± 1.9% versus *Ldlr*$^{-/-}$ 8.2 ± 1.5%, $P < 0.01$; Figure 4). These data demonstrated that the atherosclerotic lesions induced by IHC evolved faster and to a more severe extent in *ApoE*$^{-/-}$ mice as compared with *Ldlr*$^{-/-}$ mice. In addition, under the RA condition, the extent of PA lesions was more severe in *ApoE*$^{-/-}$ than in *Ldlr*$^{-/-}$ mice after 8 weeks of treatment (PA RA 8 wk, *ApoE*$^{-/-}$ 8.0 ± 2.8% versus *Ldlr*$^{-/-}$ 2.1 ± 0.2%, $P < 0.05$), indicating that the *ApoE*$^{-/-}$ mice were still able to develop more extensive lesions in the absence of IHC.

Contribution of Microbes and Their Metabolite TMA to Atherosclerosis

Accumulating evidence suggests that the metabolism of dietary components (e.g., choline enriched in an HFD) by gut flora may have a substantial influence on atherogenesis. Hazen's group has demonstrated that DMB, a nonlethal inhibitor of gut microbial TMA production, reduces the formation of atherosclerotic lesions in *ApoE*$^{-/-}$ mice (10). Here, we used DMB to evaluate the involvement of microbes and their metabolite TMA in

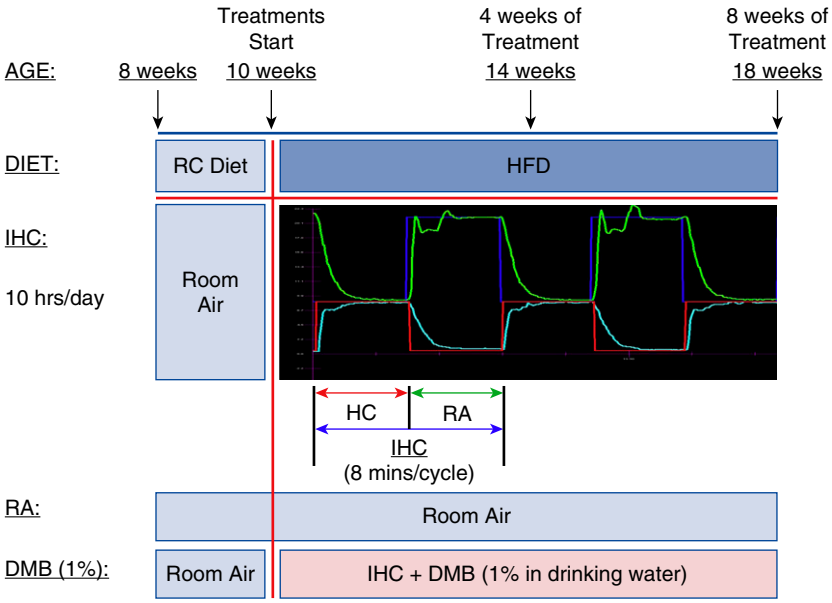

Figure 1. Schematic illustration of the treatment paradigm. Groups of 8-week-old male mice were transferred to the treatment room for 2 weeks of acclimatization with room air (RA) and regular chow (RC). At 10 weeks of age, the mice were switched to a high-fat diet (HFD) and treated with or without intermittent hypoxia and hypercapnia (IHC). The IHC treatment groups were exposed to IHC for 10 hours/day in the light cycle for 4 or 8 weeks. (The *blue line* indicates the O_2 set point and the *green line* shows the actual level of O_2. The *red line* indicates the CO_2 set point and the *light blue line* shows the actual level of CO_2.) The control groups remained in RA for the same period. 3,3-Dimethyl-1-butanol (DMB; 1.0%, vol/vol) was provided in the drinking water of *ApoE*$^{-/-}$ mice under the IHC condition for 8 weeks.

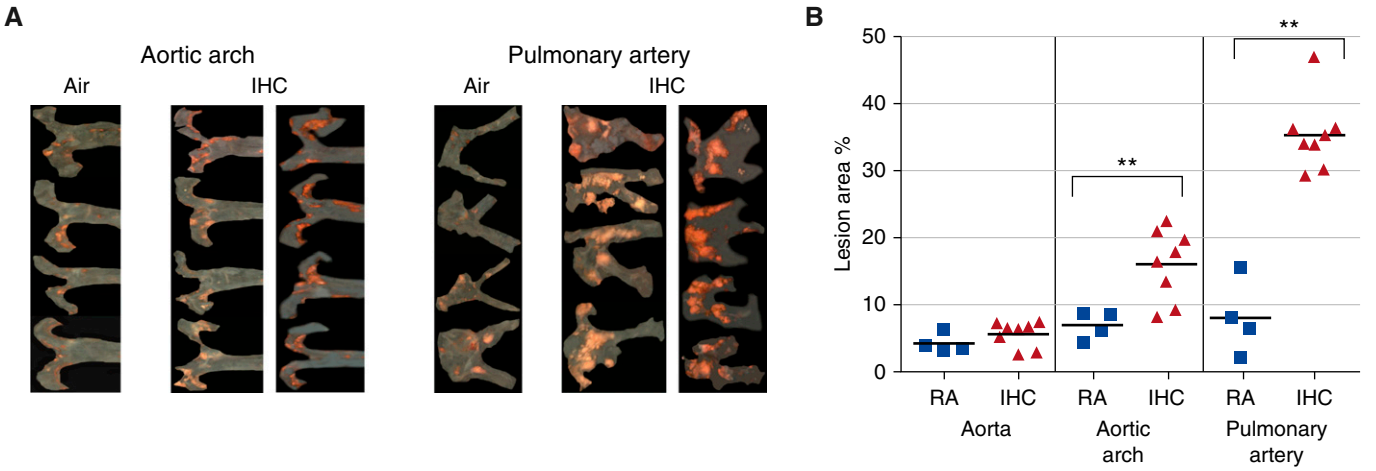

Figure 2. Atherosclerotic lesion formation in *ApoE*$^{-/-}$ mice on a high-fat diet. *ApoE*$^{-/-}$ mice were exposed to either RA or IHC for 8 weeks. *En face* lesions were quantified in the aorta, aortic arch, and pulmonary arteries (PAs) as described in Materials and Methods. (*A*) Sudan IV–stained aortic arch and PA of each individual mouse examined. (*B*) Quantitative analysis. The *x-axis* shows the different areas of the blood vessels (IHC versus RA). The *y-axis* depicts % of lesion area for all mice in the experimental protocols; $n = 4$ for RA and 8 for IHC; $^{**}P < 0.01$. IHC significantly accelerated atherosclerotic lesion formation in the aortic arch and PA of *ApoE*$^{-/-}$ mice.

IHC-induced atherosclerosis, a model for OSA.

We examined the effect of chronic DMB exposure (1% in drinking water for 8 wk) on the development of atherosclerosis by IHC in the *ApoE*$^{-/-}$ mice. As reported above, IHC induced a marked increase in lesion formation of the aortic arch and PA. Although DMB in the drinking water significantly reduced the observed IHC-induced atherosclerotic lesions in the PA (but not in the aortic arch), it did not completely abolish these IHC-enhanced lesions (PA 8 wk, IHC DMB 25.6 ± 2.6% versus IHC 35.4 ± 1.9% [$P < 0.01$] or versus RA 8.0 ± 2.8% [$P < 0.01$]; Figure 5). These data demonstrate that gut microbes and their metabolite TMA play an important role in mediating IHC-induced atherosclerosis of the PA.

Discussion

OSA is a prevalent sleep disorder characterized by repetitive episodes of complete or partial airway obstruction, resulting in apneas or hypopneas. OSA is often accompanied by loud snoring, intermittent arterial oxygen desaturation and hypercapnia, sleep fragmentation, sleep arousal, daytime sleepiness, and cognitive

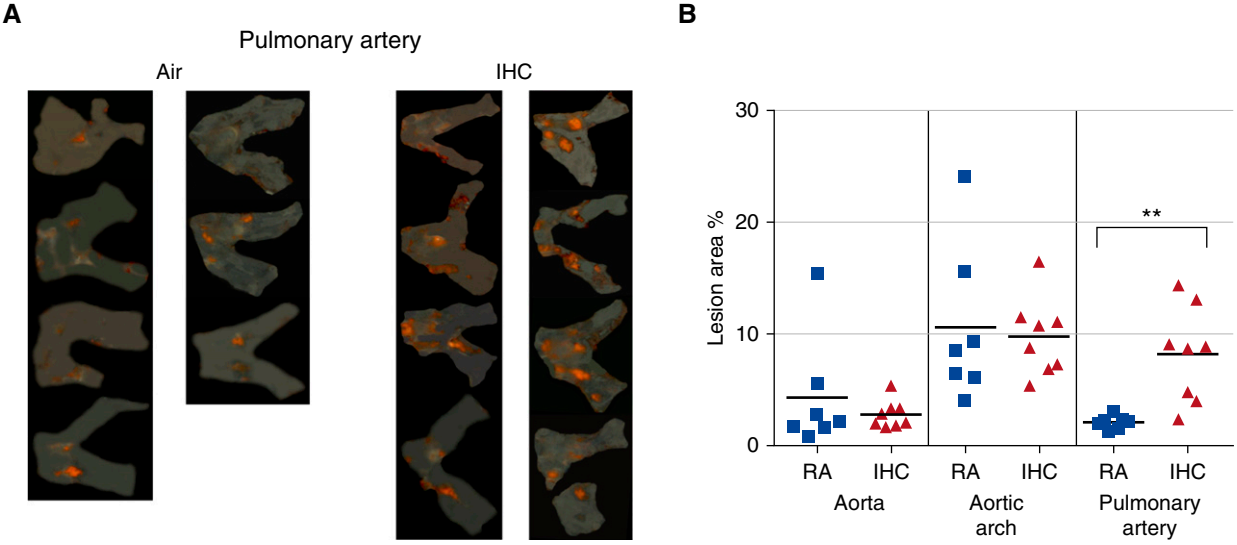

Figure 3. Atherosclerotic lesion formation in *Ldlr*$^{-/-}$ mice on a high-fat diet. *Ldlr*$^{-/-}$ mice were exposed to either RA or IHC for 8 weeks. *En face* lesions were quantified in the aorta, aortic arch, and PAs as described in Materials and Methods. (*A*) Sudan IV–stained PA of each individual mouse examined. (*B*) Quantitative analysis. The *x-axis* shows the different areas of the blood vessels (IHC versus RA). The *y-axis* depicts % of lesion area for all mice in the experimental protocols; $n = 7$ for RA and 8 for IHC; $^{**}P < 0.01$. IHC significantly accelerated atherosclerotic lesion formation in the PA of *Ldlr*$^{-/-}$ mice.

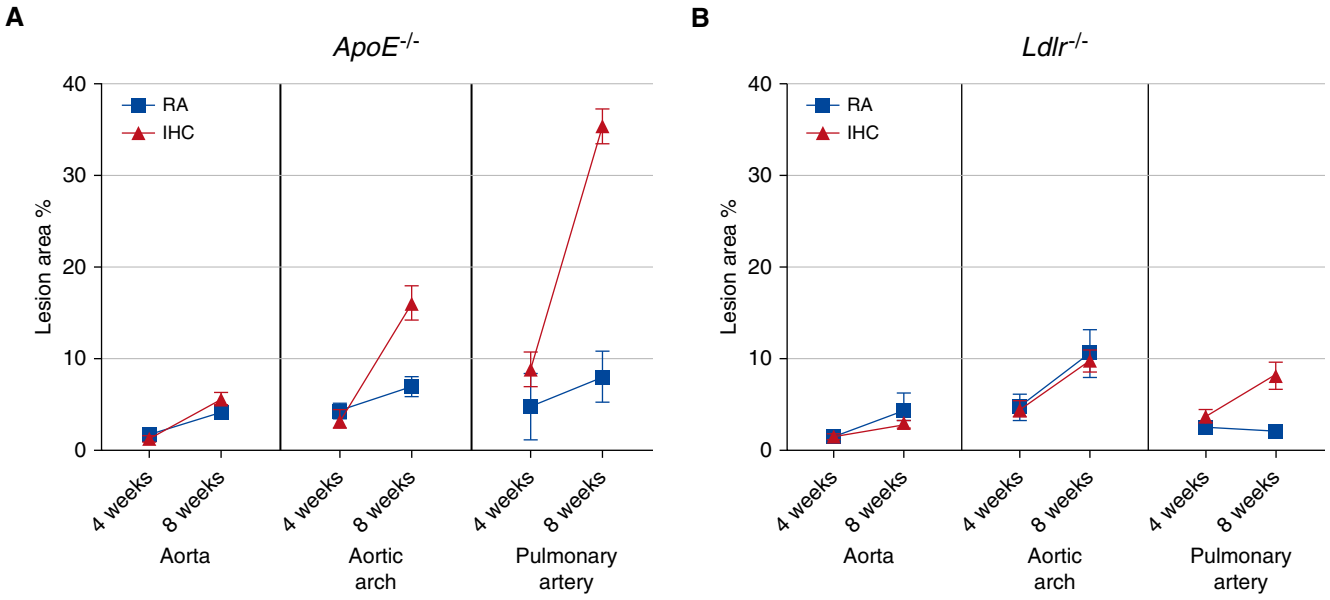

Figure 4. Lesion progression from 4 weeks to 8 weeks of treatment in RA and IHC conditions. (*A*) *ApoE*$^{-/-}$ mice. (*B*) *Ldlr*$^{-/-}$ mice. The data are presented as means ± SEM. *Blue*: RA controls; *red*: IHC-treated mice. In *ApoE*$^{-/-}$ mice, the lesions evolved faster in the aortic arch and PA of IHC groups. In *Ldlr*$^{-/-}$ mice, IHC promoted only PA lesions and had no impact on the aorta or aortic arch. No lesion progression was detected in the PA from 4 to 8 weeks under RA. *ApoE*, apolipoprotein E; *Ldlr*, low density lipoprotein receptor.

dysfunction. Chronic IH is a prominent feature of OSA pathophysiology. Several animal paradigms have been developed to understand the deleterious effect of chronic IH in patients with OSA (23). Spontaneous and surgical/mechanical animal models are labor intensive, and are limited by the number and size of the animals and/or the invasiveness of the procedures used. The most commonly used experimental IH protocol is the introduction of low O_2 by rapid delivery of a hypoxic mixture to an airtight chamber followed by flushing with normoxic RA. Reducing the ambient chamber oxygen to 5–10% results in an SaO_2 of 60–80% (23). IH exposure is given during daytime when rodents generally sleep. The atherosclerosis induced by IH in these mouse models is similar to that observed in patients with OSA. Because each breathing pause of sleep apnea can last

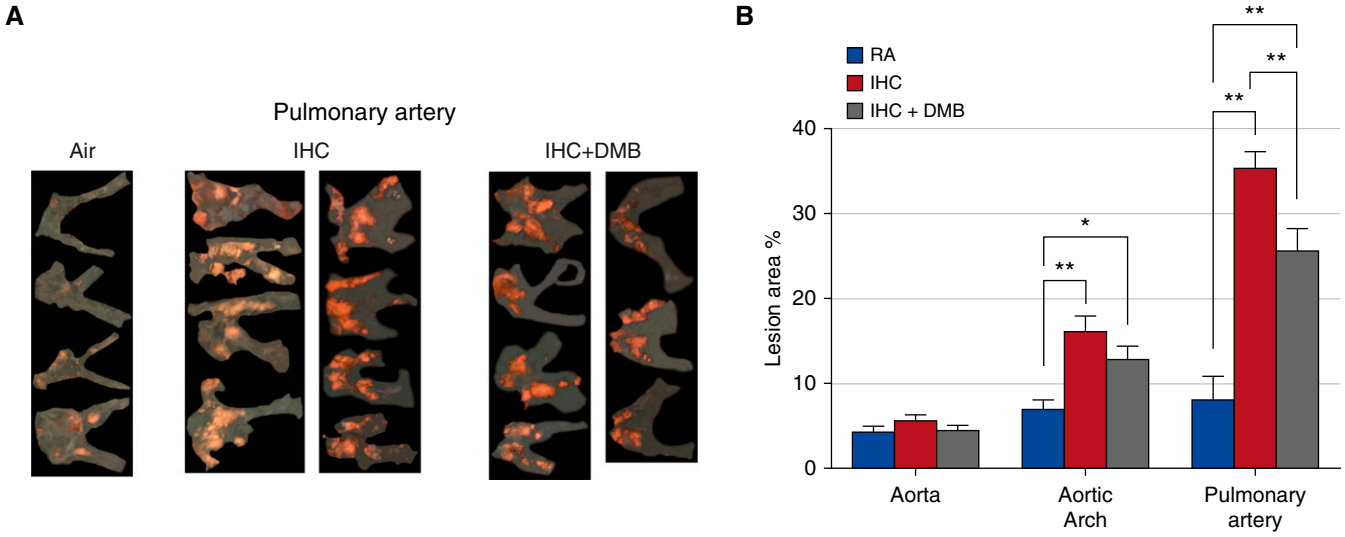

Figure 5. Effect of DMB on IHC-induced atherosclerosis. *ApoE*$^{-/-}$ mice were exposed to RA, IHC, or IHC plus DMB for 8 weeks. *En face* lesions were quantified in the aorta, aortic arch, and PAs as described in Materials and Methods. (*A*) Sudan IV–stained PA of each individual mouse examined. (*B*) Quantitative analysis. The *x-axis* shows the different areas of the blood vessels (RA versus IHC versus IHC+DMB). The *y-axis* depicts % of lesion area; $n = 4$ for RA, 8 for IHC, and 7 for IHC+DMB. Values are means ± SEM; $^{**}P < 0.01$, $^{*}P < 0.05$. DMB treatment partially reduced the size of IHC-enhanced lesions in the PA.

from a few seconds to minutes (24), we chose to use a severe IH treatment (minutes) in the present study. We also included hypercapnia in our experimental protocol to better simulate the oscillations of O_2 and CO_2 in patients with OSA.

We previously found that IHC induced an unusual and dramatic accumulation of lesions in the pulmonary root and PAs of *Ldlr*$^{-/-}$ mice (9). However, a published study of *ApoE*$^{-/-}$ mice exposed only to IH lacked a description of the involvement of the PA vascular system (25). To determine whether PA lesions are a unique phenomenon of *Ldlr*$^{-/-}$ mice or the result of differences in exposure (IH versus IHC), we examined the aorta and PA in both types of mice and exposed them to IHC, to better mimic the pathophysiology of OSA.

We made several important observations. First, an 8-week IHC exposure expedited HFD-induced formation of atherosclerosis in both the PA and aortic arch of *ApoE*$^{-/-}$ mice, but only in the PA of *Ldlr*$^{-/-}$ mice. To our knowledge, we are the first to report that IHC accelerated atherosclerotic lesion formation in the PA trunk and its proximal branches in both *ApoE*$^{-/-}$ and *Ldlr*$^{-/-}$ mice (Ref. 9 and the present study). The significant increase in the lesions was observed after 8 weeks of IHC treatment. Atherosclerotic PA lesions were previously described in *ApoE*$^{-/-}$/*Ldlr*$^{-/-}$ double-knockout mice by Langheinrich and colleagues (26). However, it took longer in that study for lesions to be evident (at the age of 80 weeks). Their data and ours suggest that IHC combined with HFD accelerates the progression of atherosclerosis. In humans, atherosclerosis in the PA has been reported in patients with chronic obstructive pulmonary disease (27), and has been associated with hypertensive pulmonary vascular disease (28). PA atherosclerosis was shown to be a significant predictor of aortic atherosclerosis, right-ventricular hypertrophy, and pulmonary embolization (28). In several studies involving *ApoE*$^{-/-}$ mice, IH alone (no hypercapnia) with HFD was demonstrated to induce aortic atherosclerosis (25, 29–31), and the authors did not mention or report any evidence of PA involvement. However, by combining IHC and HFD, we detected not only aortic atherosclerosis but also dramatic PA atherosclerosis. Therefore, it is possible that intermittent hypercapnia may play a crucial role in promoting the evolution of PA atherosclerosis. Hypercapnia has both protective and deleterious effects (32). On the one hand, hypercapnia can inhibit hypoxia pulmonary vascular remodeling (33) and prevent hypoxia-induced pulmonary hypertension (34). On the other hand, hypercapnia injures alveolar epithelial cells (35) and impairs alveolar fluid reabsorption (36). Carbon dioxide also interacts with both reactive nitrogen and reactive oxygen species (37).

In *Ldlr*$^{-/-}$ mice, IHC had no impact on the progression of aortic atherosclerosis, in contrast to what was observed for *ApoE*$^{-/-}$ mice. Although a marked increase in plasma lipids was noted in response to HFD in *Ldlr*$^{-/-}$ mice, there were no differences in total plasma cholesterol or triglyceride levels between IHC and RA controls after 8 weeks of treatment (9). It is interesting to note that mice exposed to IHC, even with reduced body weights and less high-fat food intake, formed more lesions in the PA than the RA control mice. Collectively, these findings imply that IHC promotes atherosclerosis formation in PA via mechanisms other than hyperlipidemia in *Ldlr*$^{-/-}$ mice. Conversely, IH alone induced hyperlipidemia in *ApoE*$^{-/-}$ mice (25, 30, 31). Whether the distinct effects of IHC on the aorta in *ApoE*$^{-/-}$ mice compared with *Ldlr*$^{-/-}$ mice are attributable to the lipoproteins driving the inflammatory process or to hypercapnia, or are intrinsic to the different functions of ApoE and Ldlr, is still unclear.

Second, atherosclerotic lesions developed faster and to a more severe extent in *ApoE*$^{-/-}$ mice compared with *Ldlr*$^{-/-}$ mice. Despite the fact that *ApoE*$^{-/-}$ and *Ldlr*$^{-/-}$ mice are widely used to study atherosclerosis, only a limited number of studies have compared them under the same experimental conditions (38). In our well-controlled experiments, *ApoE*$^{-/-}$ and *Ldlr*$^{-/-}$ mice were maintained in the same vivarium (i.e., microbiome effects), fed the same HFD, and sampled from the same arterial sites of male mice only and at the same times during the evolution of lesions. *ApoE*$^{-/-}$ and *Ldlr*$^{-/-}$ mice have shown some similarities but also exhibit major differences in atherogenesis. They all developed atherosclerosis to a certain extent after the HFD under both RA and IHC conditions. The extent of lesions after 8 weeks of IHC treatment was remarkably higher in *ApoE*$^{-/-}$ mice than in *Ldlr*$^{-/-}$ mice. IHC affected lesion formation in both the aortic arch and PA in *ApoE*$^{-/-}$ mice, whereas IHC affected only the PA in *Ldlr*$^{-/-}$ mice. Several possibilities may account for these differences:

(*1*) Lipoprotein profiles. *ApoE*$^{-/-}$ mice have high blood cholesterol levels (~400 mg/dl) and greatly increased levels of very-low-density lipoproteins, which are mostly apoB48-containing cholesteryl ester-rich particles, along with reduced levels of high-density lipoproteins. In contrast, *Ldlr*$^{-/-}$ mice have moderately increased blood cholesterol levels (~200–275 mg/dl) and the predominant lipoproteins are apoB100-containing low-density lipoproteins, along with elevated high-density lipoprotein levels (38). The influx of apoB-containing lipoproteins into the subendothelial space at injured vascular sites is the initiating process of atherogenesis (39). The size of the lipoproteins, as well as their vascular wall permeability, composition, and association with matrix components, determine their retention in the subendothelial space (38). Thus, different lipoprotein patterns may result in distinct lesion formation.

(*2*) Vascular inflammation and oxidative stress. Previous studies have shown that multiple mechanisms may contribute to exacerbated atherosclerosis during chronic intermittent hypoxia, including proatherogenic dyslipidemia, hypertension, vascular inflammation, and oxidative stress (25, 29–31). In addition to its capacity to lower plasma lipids, ApoE serves antiinflammatory and antioxidative functions, such as polarizing macrophages from the proinflammatory M1 subset to the antiinflammatory M2 subset (40), reducing isoprostane generation and atherosclerotic lesion formation (41), and promoting cholesterol efflux from macrophages (38). Ldlr does not share these functions.

(*3*) Different atherogenic signaling pathways. Further investigations will be necessary to elucidate the mechanistic basis of the difference between the functions of the PA and the aorta, but in theory it may reflect differences in their respective endothelial cells and their response to IHC.

Third, DMB significantly attenuated IHC-induced PA atherosclerosis, but did not completely eliminate IHC-induced lesion formation. There is a growing recognition that gut microbes take part in

the host metabolism and contribute to cardiometabolic phenotypes. For example, TMAO, a gut microbial metabolite, has been demonstrated to be atherogenic. TMAO arises from gut microbiota metabolism after ingestion of TMA-containing dietary nutrients such as phosphatidylcholine, choline, and carnitine. Multiple clinical studies have shown that elevated plasma TMAO levels are associated with an increased burden of atherosclerotic lesions and risk for cardiovascular disease (11, 14, 15, 17, 42). Functional studies revealed that TMAO stimulates the expression of the LDL scavenger receptors SRA and CD36 in macrophages, thereby promoting LDL uptake and the formation of foam cells. In hepatocytes, TMAO suppresses bile acid synthesis from cholesterol and reduces the expression of bile acid transporters, which may increase the risk for atherosclerosis (43). DMB, a blocker of microbial TMA lyases, inhibits TMA production and reduces plasma TMAO levels (10). Interestingly, we found that DMB partially alleviated the atherosclerotic lesions in the PA of IHC-exposed $ApoE^{-/-}$ mice. The results indicate that the gut microbes and their metabolites TMA and TMAO play an important role in IHC-induced atherosclerosis of the PA.

We have profiled gut microbiota and metabolites in fecal material using multi-omics–based approaches (16S sequencing and metabolomics) in both IHC and RA groups. Our preliminary data show that the gut microbiome under IHC is indeed significantly different from that of RA control mice, and the biological effect of treatment is greater than the confounding effect of housing conditions (44).

It is of note that DMB could not restore the lesions to those associated with RA exposure. Our data then suggest that other mechanisms contribute to this process. For example, (*1*) IHC causes pulmonary arteriolar vasoconstriction and pulmonary arterial hypertension, which might lead to damage of endothelial cells, initiating atherosclerosis formation; (*2*) IHC has also been shown to result in dyslipidemia, oxidative stress, and inflammation (45–50), which make patients with OSA more susceptible to atherosclerosis; and (*3*) other microbes and their metabolites that are not blocked by DMB may be involved. For instance, lipopolysaccharide (LPS), released by commensal bacteria such as *Firmicutes* sp. and *Bacteroidetes* sp. in the gut, may also be a key participant in the pathogenesis of atherosclerosis. IHC may change the gut microbiota and enhance the LPS load. LPS is recognized by Toll-like receptor 4 and exerts proatherogenic effects by activating inflammatory signaling pathways, modulating the host immune response and lipid metabolism, and promoting permeabilization of the intestinal wall (43).

In summary, we have established a model of OSA to study the pathological consequences of an OSA surrogate, namely, IHC. We found that IHC accelerated atherosclerosis in both the PA and aortic arch of $ApoE^{-/-}$ mice, but only in the PA of $Ldlr^{-/-}$ mice. $ApoE^{-/-}$ mice developed more extensive and severe atherosclerotic lesions than $Ldlr^{-/-}$ mice. DMB partially blocked IHC-induced atherosclerosis of PA and might be a promising therapeutic drug. ■

Author disclosures are available with the text of this article at www.atsjournals.org.

Acknowledgments: The authors thank Jennifer Pattison and Karen Bowden from the Witztum laboratory at the University of California San Diego for their technical assistance.

References

1. McNicholas WT, Bonsignore MR. Sleep apnoea as an independent risk factor for cardiovascular disease: current evidence, basic mechanisms and research priorities. *Eur Respir J* 2007;29: 156–178.
2. Peker Y, Kraiczi H, Hedner J, Loth S, Johansson A, Bende M. An independent association between obstructive sleep apnoea and coronary artery disease. *Eur Respir J* 1999;14:179–184.
3. Lavie P, Lavie L. Cardiovascular morbidity and mortality in obstructive sleep apnea. *Curr Pharm Des* 2008;14:3466–3473.
4. Gunnarsson SI, Peppard PE, Korcarz CE, Barnet JH, Aeschlimann SE, Hagen EW, Young T, Hla KM, Stein JH. Obstructive sleep apnea is associated with future subclinical carotid artery disease: thirteen-year follow-up from the Wisconsin sleep cohort. *Arterioscler Thromb Vasc Biol* 2014;34:2338–2342.
5. Lee W, Nagubadi S, Kryger MH, Mokhlesi B. Epidemiology of obstructive sleep apnea: a population-based perspective. *Expert Rev Respir Med* 2008;2:349–364.
6. Zhang SH, Reddick RL, Piedrahita JA, Maeda N. Spontaneous hypercholesterolemia and arterial lesions in mice lacking apolipoprotein E. *Science* 1992;258:468–471.
7. Plump AS, Smith JD, Hayek T, Aalto-Setala K, Walsh A, Verstuyft JG, Rubin EM, Breslow JL. Severe hypercholesterolemia and atherosclerosis in apolipoprotein E-deficient mice created by homologous recombination in ES cells. *Cell* 1992;71:343–353.
8. Ishibashi S, Brown MS, Goldstein JL, Gerard RD, Hammer RE, Herz J. Hypercholesterolemia in low density lipoprotein receptor knockout mice and its reversal by adenovirus-mediated gene delivery. *J Clin Invest* 1993;92:883–893.
9. Douglas RM, Bowden K, Pattison J, Peterson AB, Juliano J, Dalton ND, Gu Y, Alvarez E, Imamura T, Peterson KL, *et al*. Intermittent hypoxia and hypercapnia induce pulmonary artery atherosclerosis and ventricular dysfunction in low density lipoprotein receptor deficient mice. *J Appl Physiol* 1985;2013:1694–1704.
10. Wang Z, Roberts AB, Buffa JA, Levison BS, Zhu W, Org E, Gu X, Huang Y, Zamanian-Daryoush M, Culley MK, *et al*. Non-lethal inhibition of gut microbial trimethylamine production for the treatment of atherosclerosis. *Cell* 2015;163:1585–1595.
11. Senthong V, Li XMS, Hudec T, Coughlin J, Wu YP, Levison B, Wang ZN, Hazen SL, Tang WHW. Plasma trimethylamine n-oxide, a gut microbe-generated phosphatidylcholine metabolite, is associated with atherosclerotic burden. *J Am Coll Cardiol* 2016;67:2620–2628.
12. Koeth RA, Wang Z, Levison BS, Buffa JA, Org E, Sheehy BT, Britt EB, Fu X, Wu Y, Li L, *et al*. Intestinal microbiota metabolism of L-carnitine, a nutrient in red meat, promotes atherosclerosis. *Nat Med* 2013;19: 576–585.
13. Mente A, Chalcraft K, Ak H, Davis AD, Lonn E, Miller R, Potter MA, Yusuf S, Anand SS, McQueen MJ. The relationship between trimethylamine-n-oxide and prevalent cardiovascular disease in a multiethnic population living in Canada. *Can J Cardiol* 2015;31:1189–1194.
14. Tang WH, Wang Z, Levison BS, Koeth RA, Britt EB, Fu X, Wu Y, Hazen SL. Intestinal microbial metabolism of phosphatidylcholine and cardiovascular risk. *N Engl J Med* 2013;368:1575–1584.
15. Tang WH, Wang Z, Fan Y, Levison B, Hazen JE, Donahue LM, Wu Y, Hazen SL. Prognostic value of elevated levels of intestinal microbe-generated metabolite trimethylamine-*N*-oxide in patients with heart failure: refining the gut hypothesis. *J Am Coll Cardiol* 2014;64:1908–1914.
16. Troseid M, Ueland T, Hov JR, Svardal A, Gregersen I, Dahl CP, Aakhus S, Gude E, Bjorndal B, Halvorsen B, *et al*. Microbiota-dependent metabolite trimethylamine-*N*-oxide is associated with disease severity and survival of patients with chronic heart failure. *J Intern Med* 2015;277:717–726.
17. Wang Z, Klipfell E, Bennett BJ, Koeth R, Levison BS, Dugar B, Feldstein AE, Britt EB, Fu X, Chung YM, *et al*. Gut flora metabolism of phosphatidylcholine promotes cardiovascular disease. *Nature* 2011; 472:57–63.

18. Moreno-Indias I, Torres M, Montserrat JM, Sanchez-Alcoholado L, Cardona F, Tinahones FJ, Gozal D, Poroyko VA, Navajas D, Queipo-Ortuno MI, *et al*. Intermittent hypoxia alters gut microbiota diversity in a mouse model of sleep apnoea. *Eur Respir J* 2015;45:1055–1065.
19. Xue J, Zhou D, Poulsen O, Imamura T, Hsiao Y-H, Malhotra A, Dorrestein P, Knight R, Haddad GG. Intermittent hypoxia and hypercapnia accelerate aorta and pulmonary artery atherosclerosis, partially mediated via trimethylamine-oxide (TMAO) in both $ApoE^{-/-}$ and $Ldlr^{-/-}$ mice on high fat diet. *FASEB J* 2017;31(no. 1 Suppl): lb636.
20. Piedrahita JA, Zhang SH, Hagaman JR, Oliver PM, Maeda N. Generation of mice carrying a mutant apolipoprotein E gene inactivated by gene targeting in embryonic stem cells. *Proc Natl Acad Sci USA* 1992;89:4471–4475.
21. Douglas RM, Xue J, Chen JY, Haddad CG, Alper SL, Haddad GG. Chronic intermittent hypoxia decreases the expression of Na/H exchangers and HCO3-dependent transporters in mouse CNS. *J Appl Physiol* 1985;2003:292–299.
22. Schneider CA, Rasband WS, Eliceiri KW. NIH Image to ImageJ: 25 years of image analysis. *Nat Methods* 2012;9:671–675.
23. Sforza E, Roche F. Chronic intermittent hypoxia and obstructive sleep apnea: an experimental and clinical approach. *Hypoxia (Auckl)* 2016; 4:99–108.
24. National Heart, Blood, and Lung Institute. Health information for the public. What is sleep apnea? [Accessed 2017 Jun 1]. Available from: https://www.nhlbi.nih.gov/health/health-topics/topics/sleepapnea/
25. Jun J, Reinke C, Bedja D, Berkowitz D, Bevans-Fonti S, Li J, Barouch LA, Gabrielson K, Polotsky VY. Effect of intermittent hypoxia on atherosclerosis in apolipoprotein E-deficient mice. *Atherosclerosis* 2010;209:381–386.
26. Langheinrich AC, Michniewicz A, Bohle RM, Ritman EL. Vasa vasorum neovascularization and lesion distribution among different vascular beds in ApoE(−/−)/LDL(−/−) double knockout mice. *Atherosclerosis* 2007;191:73–81.
27. Russo A, De Luca M, Vigna C, De Rito V, Pacilli M, Lombardo A, Armillotta M, Fanelli R, Loperfido F. Central pulmonary artery lesions in chronic obstructive pulmonary disease: a transesophageal echocardiography study. *Circulation* 1999;100:1808–1815.
28. Moore GW, Smith RR, Hutchins GM. Pulmonary artery atherosclerosis: correlation with systemic atherosclerosis and hypertensive pulmonary vascular disease. *Arch Pathol Lab Med* 1982;106: 378–380.
29. Arnaud C, Poulain L, Levy P, Dematteis M. Inflammation contributes to the atherogenic role of intermittent hypoxia in apolipoprotein-E knock out mice. *Atherosclerosis* 2011;219:425–431.
30. Li RC, Haribabu B, Mathis SP, Kim J, Gozal D. Leukotriene B4 receptor-1 mediates intermittent hypoxia-induced atherogenesis. *Am J Respir Crit Care Med* 2011;184:124–131.
31. Savransky V, Nanayakkara A, Li J, Bevans S, Smith PL, Rodriguez A, Polotsky VY. Chronic intermittent hypoxia induces atherosclerosis. *Am J Respir Crit Care Med* 2007;175:1290–1297.
32. Azzam ZS, Sharabi K, Guetta J, Bank EM, Gruenbaum Y. The physiological and molecular effects of elevated CO2 levels. *Cell Cycle* 2010;9:1528–1532.
33. Ooi H, Cadogan E, Sweeney M, Howell K, O'Regan RG, McLoughlin P. Chronic hypercapnia inhibits hypoxic pulmonary vascular remodeling. *Am J Physiol Heart Circ Physiol* 2000;278:H331–H338.
34. Kantores C, McNamara PJ, Teixeira L, Engelberts D, Murthy P, Kavanagh BP, Jankov RP. Therapeutic hypercapnia prevents chronic hypoxia-induced pulmonary hypertension in the newborn rat. *Am J Physiol Lung Cell Mol Physiol* 2006;291:L912–L922.
35. Lang JD, Chumley P, Eiserich JP, Estevez A, Bamberg T, Adhami A, Crow J, Freeman BA. Hypercapnia induces injury to alveolar epithelial cells via a nitric oxide-dependent pathway. *Am J Physiol Lung Cell Mol Physiol* 2000;279:L994–L1002.
36. Vadasz I, Dada LA, Briva A, Trejo HE, Welch LC, Chen J, Toth PT, Lecuona E, Witters LA, Schumacker PT, *et al*. AMP-activated protein kinase regulates CO2-induced alveolar epithelial dysfunction in rats and human cells by promoting Na,K-ATPase endocytosis. *J Clin Invest* 2008;118:752–762.
37. Vesela A, Wilhelm J. The role of carbon dioxide in free radical reactions of the organism. *Physiol Res* 2002;51:335–339.
38. Getz GS, Reardon CA. Do the Apoe(−/−) and Ldlr(−/−) mice yield the same insight on atherogenesis? *Arterioscler Thromb Vasc Biol* 2016; 36:1734–1741.
39. Tabas I, Williams KJ, Boren J. Subendothelial lipoprotein retention as the initiating process in atherosclerosis—update and therapeutic implications. *Circulation* 2007;116:1832–1844.
40. Baitsch D, Bock HH, Engel T, Telgmann R, Muller-Tidow C, Varga G, Bot M, Herz J, Robenek H, von Eckardstein A, *et al*. Apolipoprotein E induces antiinflammatory phenotype in macrophages. *Arterioscler Thromb Vasc Biol* 2011;31:1160–1168.
41. Tangirala RK, Pratico D, FitzGerald GA, Chun S, Tsukamoto K, Maugeais C, Usher DC, Pure E, Rader DJ. Reduction of isoprostanes and regression of advanced atherosclerosis by apolipoprotein E. *J Biol Chem* 2001;276:261–266.
42. Gregory JC, Buffa JA, Org E, Wang Z, Levison BS, Zhu W, Wagner MA, Bennett BJ, Li L, DiDonato JA, *et al*. Transmission of atherosclerosis susceptibility with gut microbial transplantation. *J Biol Chem* 2015; 290:5647–5660.
43. Chistiakov DA, Bobryshev YV, Kozarov E, Sobenin IA, Orekhov AN. Role of gut microbiota in the modulation of atherosclerosis-associated immune response. *Front Microbiol* 2015;6:671.
44. Tripathi A, Meehan MJ, Humphrey G, Zhou D, Xue J, Poulsen O, Sanders J, Haddad GG, Dorrestein PC, Knight R. Atherosclerosis, sleep apnea and obesity: evidence of a microbiome connection. Presented at the Fifth Annual Winter Q-Bio Meeting. February 21–24, 2017, Koloa (Kauai), Hawaii. p. 131
45. Drager LF, Bortolotto LA, Lorenzi MC, Figueiredo AC, Krieger EM, Lorenzi-Filho G. Early signs of atherosclerosis in obstructive sleep apnea. *Am J Respir Crit Care Med* 2005;172:613–618.
46. Kasasbeh E, Chi DS, Krishnaswamy G. Inflammatory aspects of sleep apnea and their cardiovascular consequences. *South Med J* 2006; 99:58–67.
47. Lavie L, Vishnevsky A, Lavie P. Evidence for lipid peroxidation in obstructive sleep apnea. *Sleep* 2004;27:123–128.
48. McArdle N, Hillman D, Beilin L, Watts G. Metabolic risk factors for vascular disease in obstructive sleep apnea: a matched controlled study. *Am J Respir Crit Care Med* 2007;175:190–195.
49. Robinson GV, Pepperell JC, Segal HC, Davies RJ, Stradling JR. Circulating cardiovascular risk factors in obstructive sleep apnoea: data from randomised controlled trials. *Thorax* 2004;59:777–782.
50. Tauman R, O'Brien LM, Gozal D. Hypoxemia and obesity modulate plasma C-reactive protein and interleukin-6 levels in sleep-disordered breathing. *Sleep Breath* 2007;11:77–84.